

Structural properties and liquid spinodal of water confined in a hydrophobic environment.

P. Gallo^{†*} and M. Rovere[†]

[†] *Dipartimento di Fisica, Università "Roma Tre",
and Democritos National Simulation Center,
Via della Vasca Navale 84, 00146 Roma, Italy*

We present the results of a computer simulation study of thermodynamical properties of TIP4P water confined in a hydrophobic disordered matrix of soft spheres upon supercooling. The hydrogen bond network of water appears preserved in this hydrophobic confinement. Nonetheless a reduction in the average number of hydrogen bonds due to the geometrical constraints is observed. The liquid branch of the spinodal line is calculated from 350 K down to 210 K. The same thermodynamic scenario of the bulk is found: the spinodal curve is monotonically decreasing. The line of maximum density bends avoiding a crossing of the spinodal. There is however a shift both of the line of maximum density and of the spinodal toward higher pressures and lower temperatures with respect to bulk.

PACS numbers: 61.20.Ja,64.60.My,61.20.-p

I. INTRODUCTION

The behaviour of the liquid-gas spinodal in water plays an important role in the interpretation and the determination of its complete phase diagram. In particular the related behaviours of the liquid branch of the spinodal and the line of maximum density (TMD line) in the supercooled liquid state are connected to the possible existence of a second critical point^{1,2}. Among the different interpretations of the anomalies of water at low temperatures in fact a number of experimental and computer simulation results and theoretical calculations indicate the possibility of a liquid-liquid (LL) coexistence and a second critical point^{3,4}. The low density and high density liquid phases would be in correspondence with the low density and high density amorphous forms of water below its glass transition temperature. In accordance with these hypotheses the many numerical studies performed to determine the spinodal line of bulk supercooled water agree in finding that this line is monotonically decreasing at least down to the lowest temperatures that was possible to investigate^{6,7,8,9,10,11,12,13}. Correspondingly the TMD line bends to avoid crossing the spinodal. This scenario excludes both TMD and spinodal behaviour to be responsible of the water singularities. These singularities can therefore be connected to the existence of the second critical point or to a singularity free scenario¹⁴.

An increasing amount of theoretical and experimental studies have been performed in recent years on water in confined geometries, see for example^{15,16,17,18,19,20,21,22,23,24,25,26,27,28,29,30,31,32}. Water is in fact confined in many situations of interest for biological and technological applications. In this respect the study of the modification of the phase diagram of

water induced by the perturbation of the confining environments is particularly significant. The study of water in confinement also can help to shed light on the behaviour of the bulk in the region of deep supercooling where nucleation prevents experiments to be performed in the bulk while permits very low temperatures to be reached in confinement^{21,24,25} displaying scenarios that can be connected to the bulk behaviour³³. The shift of the phase diagram due to confinement could drive the so far experimentally inaccessible zone where the second critical point is supposedly located in a region accessible to experiment. A study of ST2 water confined between smooth plates has indicated the possibility of a LL transition in confinement³¹. A recent theoretical work indicates a shift to lower temperatures, higher densities and higher pressures of the second critical point for hydrophobic confinement²⁸. Indications of a LL transition have been also found in a recent computer simulation study²² on TIP5P water confined between hydrophobic plates, a shift to lower temperature of the second critical point is also estimated.

Generally speaking solid interfaces strongly distort the HB network²⁸. In some cases an hydrophobic environment for water can be provided by the presence of an apolar solute, as in the case of aqueous solutions of rare gases, polymers or large organic molecules. When the hydrophobic units are small enough it is expected that water maintains its hydrogen bond structure^{34,35} in spite of the perturbation of the solute, this leads to the formation of water cages around the non polar solute. In this paper we explore how this hydrophobic effect influences the behaviour of the spinodal line and the TMD upon cooling in the limit of small hydrophobic units to study the case where the structure of water is preserved or only slightly modified. Since the solute-solute interaction is expected not to play an important role in comparison with the hydrogen bond and the solute-solvent interactions, in the present study we consider as a first approximation a model where few solute particles are kept fixed

*Author to whom correspondence should be addressed; e-mail: gallo@fis.uniroma3.it

to form an hydrophobic confining matrix for water. We expect this model to catch the main features of the phenomenon.

II. MODEL AND COMPUTER SIMULATION DETAILS

The water fluid is simulated with the DL_POLY package (W. Smith, T. R. Forester and I. T. Todorov, Daresbury Laboratory, UK) using the TIP4P site model³⁶. In this model three sites are arranged according to the molecular geometry. The two sites representing the hydrogens are positively charged with $q_H = 0.52$ atomic charges, each one forms a rigid bond with the site of the oxygen at distance 0.9752 \AA . The angle between the bonds is 104.52° . The site of the oxygen is neutral while a fourth site carries the negative charge of the oxygen $q_O = -2q_H$. This site is located in the same plane of the molecule at distance 0.15 \AA from the oxygen with an angle 52.26° from the OH bond. The intermolecular interactions are represented by Coulombian terms between the charged sites and a Lennard-Jones (LJ) potential between the neutral oxygen sites. The LJ parameters are given by $\sigma_O = 3.16 \text{ \AA}$ and $\epsilon_O = 0.65 \text{ kJ/mol}$.

Water is embedded in a rigid disordered array of $N_M = 6$ soft spheres. The soft spheres interact with the water oxygen sites by means of the potential

$$v_{OM}(r) = 4\epsilon_{OM} \left(\frac{\sigma_{OM}}{r} \right)^{12} \quad (1)$$

where

$$\epsilon_{OM} = \sqrt{\epsilon_O \epsilon_M} \quad (2)$$

and

$$\sigma_{OM} = \frac{1}{2} (\sigma_O + \sigma_M) \quad (3)$$

We assume $\sigma_M = 2\sigma_O$ and $\epsilon_M = 0.1\epsilon_O$. The average distance between the centers of two soft spheres is 10.5 \AA . With this size the soft spheres are far from the limit where they appear as hard wall to water. On the other end to enhance the volume excluded effects we use a pure repulsive water-spheres interaction where the parameter ϵ_M of the soft potential is taken as $0.1\epsilon_O$ to soften the repulsive ramp. The order of magnitude of the size of the spheres is close to the typical hard sphere diameter of apolar solutes^{37,38}.

The simulations are performed in the NVT ensemble with the use of a Berendsen thermostat. The potentials are truncated at 9 \AA . The corrections to the long range Coulombic interactions are taken into account with the Ewald method. The timestep used is 1 fs .

The density of water ρ is calculated on assuming that the excluded volume due to the confining spheres is approximately $V_{excl} = \pi N_M \sigma_{OM}^3 / 6$, in this way for a given number of water molecules N_w

$$\rho = \frac{N_w}{L^3 - V_{excl}} \frac{N_A}{W_{mol}} \quad (4)$$

where L is the boxlength, N_A is the Avogadro number and W_{mol} is the molar volume. In the starting configuration the water molecules are arranged with the center of mass in a cubic lattice configuration where there are voids corresponding to the random positions of the matrix spheres. In order to have enough space for the spheres the boxlength is fixed to $L = 19.25 \text{ \AA}$. Then for a given density we place in the box a number of water molecules according to Eq. 4. The range of temperatures spanned is $200 \text{ K} < T < 350 \text{ K}$ and the density range is $0.75 \text{ g/cm}^3 < \rho < 1.02 \text{ g/cm}^3$. For each density the system is melted at $T = 500 \text{ K}$ and equilibrated at several temperatures in the range indicated above. The longest runs, corresponding to the lowest temperatures investigated, lasted 10 ns . The soft spheres positions are the same for all the states simulated. We checked for an isochore that changing the disordered configuration of the soft spheres did not significantly alter the pressure values (see fig. 10).

In Fig. 1 we show a snapshot of an equilibrated configuration for $T = 300 \text{ K}$ and $\rho = 0.85 \text{ g/cm}^3$. It is

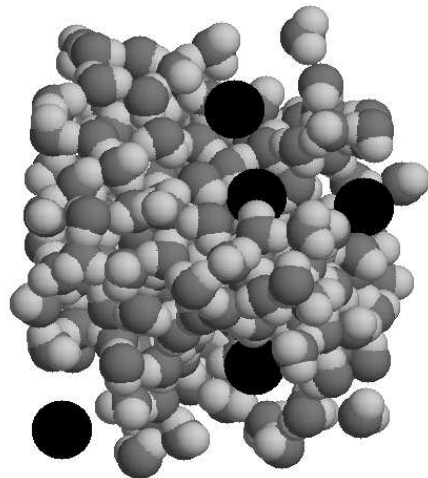


FIG. 1: Snapshot of an equilibrated configuration of the system at $T = 300 \text{ K}$ and $\rho = 0.85 \text{ g/cm}^3$. Black spheres: hydrophobic solute; gray spheres: oxygen atoms; lightgray spheres: hydrogen atoms.

evident the depletion regions around each hydrophobic sphere and the uniform distribution of water molecules elsewhere.

III. STRUCTURAL PROPERTIES

The site-site pair correlation functions have been calculated averaging the equilibrated configurations to see the effect of changing the density of water. The results for the water-water functions at ambient temperature are

reported in Fig. 2-4 for different densities and compared with the bulk for $\rho = 1 \text{ g/cm}^3$. The trend is similar to the one found in aqueous solutions of rare gases^{39,40,41}, considering that the decrease of the density in our case is equivalent to an increase of the solute concentration. The raise of OO peak in Fig. 2 with decreasing density is the signature of the enhancement of the structuring effect when less molecules are present and they can more easily approach one another. This is also evident in the behaviour of the $g_{OH}(r)$ in Fig. 3 and $g_{HH}(r)$ in Fig. 4.

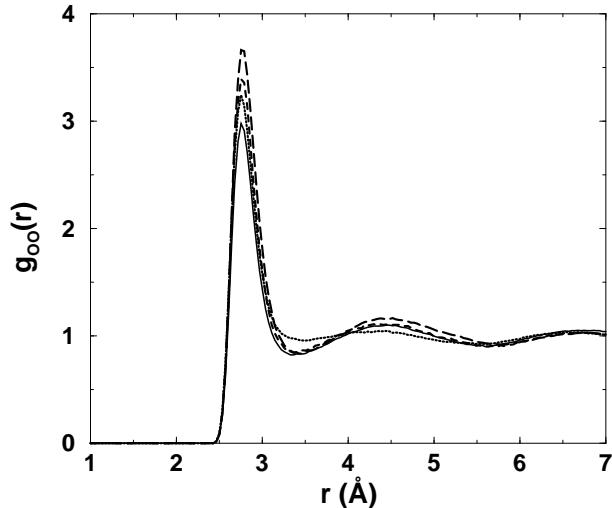


FIG. 2: Site-site pair correlation functions $g_{OO}(r)$ at $T = 300 \text{ K}$ for the confined system at densities $\rho = 1.0$ (dotted line), 0.90 (dashed line), 0.75 (long dashed line) g/cm^3 compared with the bulk at $T = 300 \text{ K}$ and $\rho = 1.0 \text{ g/cm}^3$ (solid line).

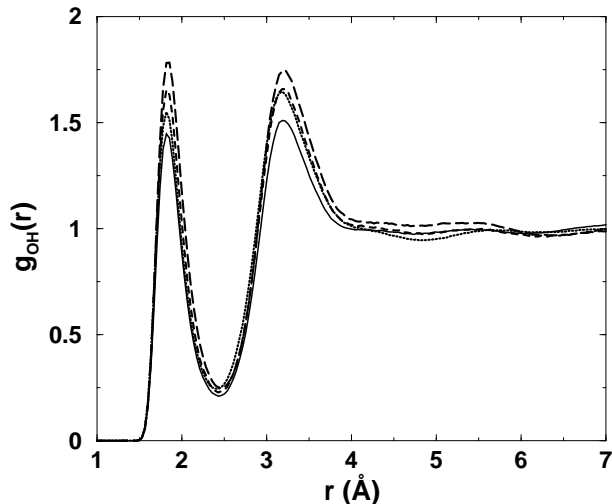


FIG. 3: Site-site pair correlation functions $g_{OH}(r)$ at the same temperature and densities as Fig. 2.

On the contrary on decreasing density the cages formed by water around the confining spheres become less struc-

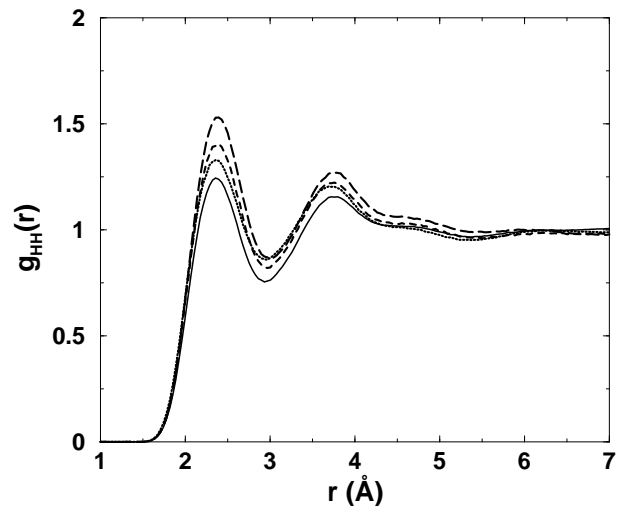


FIG. 4: Site-site pair correlation functions $g_{HH}(r)$ at the same temperature and densities as Fig. 2

tured as can be seen in Fig. 5 where the water-sphere radial distribution functions are reported for two different temperatures and different densities. The first peak of the $g_{OM}(r)$ becomes less pronounced and shifts toward higher distances, a signature of an increase of the hydrophobic repulsion at lower density. In the upper inset of Fig. 5 we show the number of nearest neighbors n_{OM} defined as follows

$$n_{OM} = 4\pi\rho c_O \int_0^{r_{min}} g_{OM}(r)r^2 dr \quad (5)$$

where r_{min} is the value of the interatomic distance at which the first minimum in $g_{OM}(r)$ is located, c_O is the concentration of oxygen atoms and ρ is the total density. We see that number of nearest neighbors n_{OM} reported in the top portion of the figure goes down as the water density decreases. In Fig. 5 it is also shown the effect of the decreasing temperature. The cage becomes more ordered and more water molecules are present on the average in the first shell around the soft spheres at high density. On lowering the density the n_{OM} reaches an asymptotic value which appears to be independent from the temperature.

The behaviour of $g_{HM}(r)$ also reported in Fig. 5 shows a similar trend as function of temperature and density. The first peak of $g_{HM}(r)$ is at the same position of the $g_{OM}(r)$ one, this indicates that the soft sphere is located interstitially in the hydrogen bond network equidistant on the average from the oxygens and hydrogens. We notice in $g_{HM}(r)$ at lower temperature for the higher density the appearance of a shoulder after the first peak, indicating that some of the O-H bonds point radially toward the second shell. Looking at the second peak of $g_{OM}(r)$ and $g_{HM}(r)$ we notice that the water molecules in the second shell are preferentially oriented with the oxygen atoms towards the sphere and the hydrogen atoms to-

wards the water similar to the trend found in aqueous solution of water and rare gases^{39,40,41}.

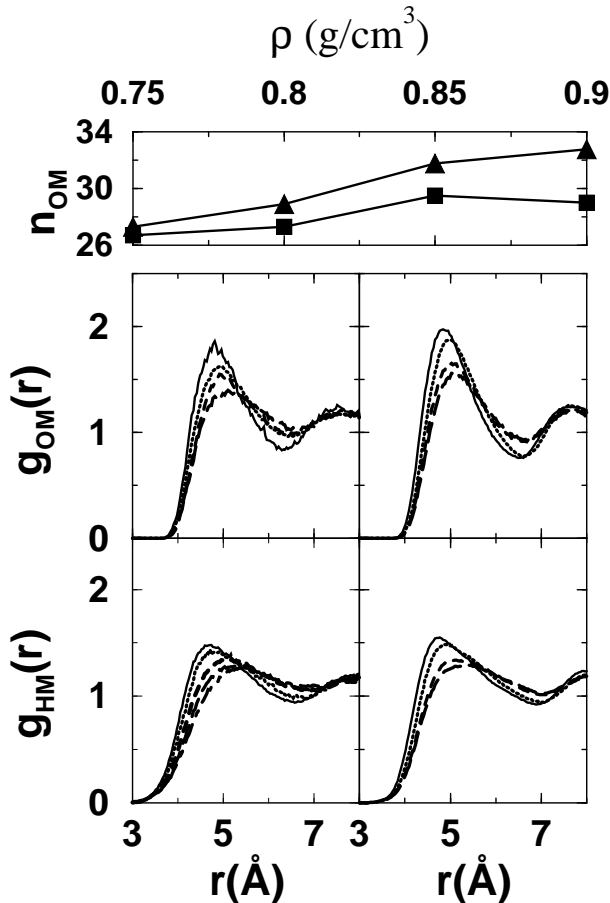


FIG. 5: Pair correlation functions $g_{OM}(r)$ (middle panel), $g_{HM}(r)$ (bottom panel) for $T = 300$ K on the left and $T = 220$ K on the right and densities $\rho = 0.90$ (solid line), 0.85 (dotted line), 0.80 (dashed line), 0.75 (long dashed line) g/cm^3 . In the top panel number of oxygen nearest neighbors n_{OM} as function of density for $T = 300$ K (full squares) and $T = 220$ K (filled triangles).

In Fig. 6 to show the effect of the temperature on the structure of water we report the $g_{OO}(r)$ for $T = 300$ K and $T = 220$ K and $\rho = 0.90$ g/cm^3 . The radial function shows maxima and minima at the same position but more pronounced at lower temperature. We notice that the $g_{OO}(r)$ for $\rho = 0.90$ g/cm^3 in the confined system is very similar to the $g_{OO}(r)$ for $\rho = 1.0$ g/cm^3 in the bulk apart from a difference in the height of the first peak. This similarity is preserved at decreasing temperatures.

To complete the analysis of the change of density on structure of water we consider the changes in the H-bond network. We define the hydrogen bond by geometric conditions. Two molecules are hydrogen bonded if the intermolecular $O \cdots O$ distance is less than 3.35 Å and the angle between the intramolecular $O - H$ vector and the intermolecular $O \cdots O$ vector is less than 30° .

In Fig. 7 it is reported the distribution function of the

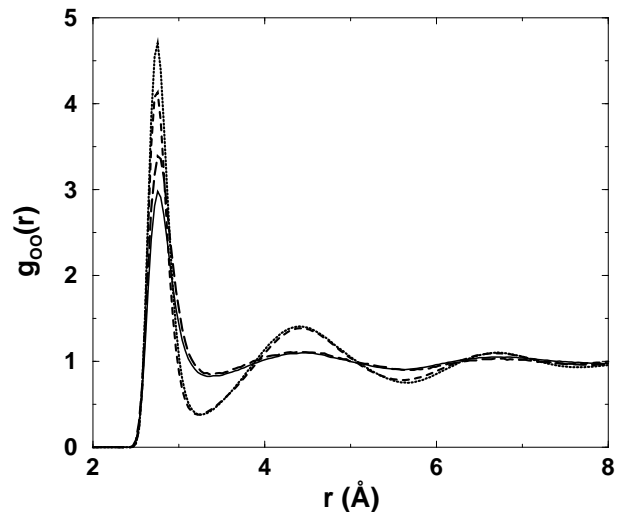


FIG. 6: Site-site pair correlation functions $g_{OO}(r)$ for the confined system at density $\rho = 0.90$ g/cm^3 and temperatures $T = 300$ K (long dashed line) and $T = 220$ K (dotted line) compared with the bulk at density $\rho = 1.0$ g/cm^3 and temperatures $T = 300$ K (solid line) and $T = 220$ K (dashed line).

average number of H-bond per molecule at two different temperatures and three densities. We have computed the average HB number for each instantaneous configuration and then we have calculated the distribution function of these average values over many configurations. We now discuss the results for the bulk at normal density compared with $\rho = 0.90$ g/cm^3 in the confined system since they appear to have a similar structure as shown above. It is evident that decreasing water density in confinement has the effect of reducing the average number of hydrogen bonds in comparison with the bulk even when $g_{OO}(r)$ are similar. At ambient temperature in confinement the distribution becomes broader and its peak position shifts to lower value with respect to bulk. These effects are enhanced by decreasing the density. At lower temperatures the H-bond distributions becomes sharper while the peak position moves toward a value close to 4

The confinement however preserves the geometry of the H-bond network. This can be deduced from the distribution of the angle θ formed by the vectors joining the oxygen atom of a central molecule and the oxygens of two nearest neighbors water molecules which are H-bonded. This distribution is reported in Fig 8. It is evident that the trend is very similar between the bulk and the confined case. On lowering the temperatures the H-bond network approaches more closely the tetrahedral ordering with a sharper distribution around the angle 104° of the TIP4P potential, while the number of interstitial molecules decreases. We note that the confined $\rho = 0.90$ g/cm^3 system has a distribution similar to the bulk $\rho = 1.0$ g/cm^3 system.

In analogy with previous work on water confined be-

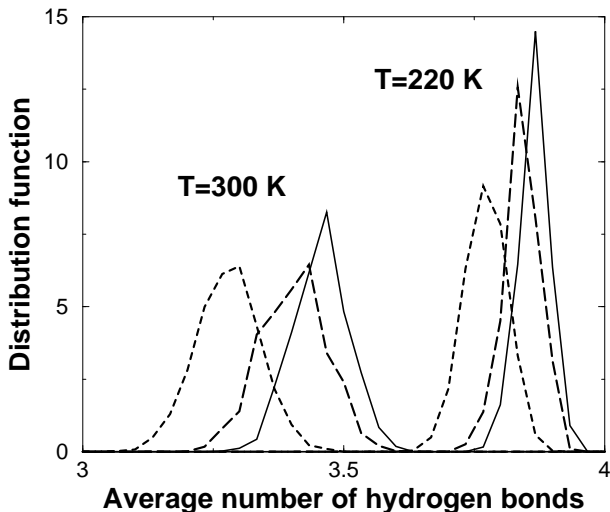


FIG. 7: Distribution functions of the average number of hydrogen bond per molecule at temperatures $T = 300$ K and $T = 220$ K for the bulk at density $\rho = 1.0$ g/cm^3 (solid line) and for the confined system at densities $\rho = 0.90$ g/cm^3 (long dashed line) and $\rho = 0.75$ g/cm^3 (dashed line).

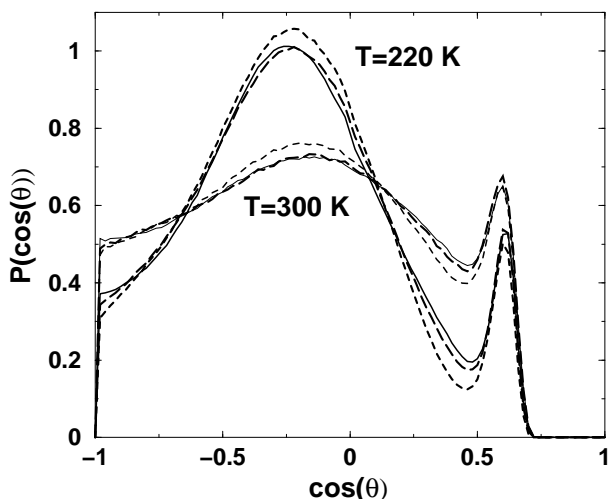


FIG. 8: Distribution functions of $\cos(\theta)$ (see text for definition) at temperatures $T = 300$ K and $T = 220$ K for the bulk at density $\rho = 1.0$ g/cm^3 (solid line) and for the confined system at densities $\rho = 0.90$ g/cm^3 (long dashed line) and $\rho = 0.75$ g/cm^3 (dashed line).

tween hydrophobic plane walls^{22,28} we find a reduction of the average number of H-bond. In our case the H-bond network does not appear to be deformed by the presence of the matrix. In the hydrophobic shells around the soft spheres water molecules maintain the H-bond network, but since they cannot form H-bonds with the neutral soft spheres the average number of hydrogen bonds is smaller compared with the bulk. As a general trend we observe that confined water seems to be equivalent to bulk water at an higher density (see Fig. 6), it is also evident that

there are not dramatic changes in the network apart from a decrease of the hydrogen bond average number.

IV. CALCULATION OF THE SPINODAL LINE

As we have shown in the previous section the soft sphere matrix does not induce large changes in the structure of water. We investigate now how the thermodynamical behaviour of confined water is changed with respect to the bulk and we will see that for thermodynamics important changes take place.

To study how the confinement in the hydrophobic matrix affects the thermodynamic stability of liquid water we calculate the liquid branch of the isotherms of our system upon cooling. From the isotherms the limit of mechanical stability can be determined in the framework of mean field theories from the divergence of the isothermal compressibility. The singularity points where

$$\left(\frac{\partial P}{\partial \rho}\right)_T = 0 \quad (6)$$

define the spinodal line. They can be obtained searching for the minima of the $P_T(\rho)$ curve. We consider here the liquid spinodal. In bulk water the liquid spinodal^{6,7,8,9,10,11,12,13} has been found to extend to the region of negative pressures.

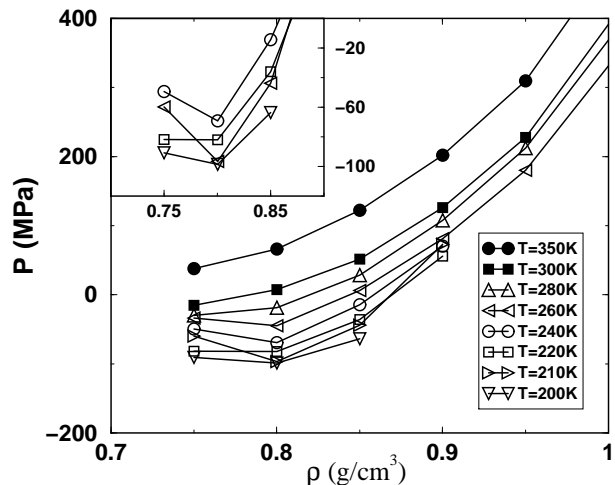


FIG. 9: Isotherms for densities ranging from $\rho = 0.75$ g/cm^3 to $\rho = 1.0$ g/cm^3 for temperatures ranging from $T = 350$ K to $T = 200$ K.

In Fig. 9 we show the isotherms of the system obtained upon cooling for densities ranging from $\rho = 0.75$ g/cm^3 to $\rho = 1.0$ g/cm^3 and temperatures from $T = 350$ K to $T = 200$ K. Below $T = 280$ K minima start appearing in the curves in correspondence with $\rho = 0.8$ g/cm^3 . In the bulk⁶ the minima appear between $\rho = 0.85 - 0.87$ g/cm^3 . From Eq. 6 we see that the minima of the isotherms represent the limit of stability of the liquid. The corresponding $P_S(T)$ spinodal line is plotted in Fig.10 to

gether with the isochores of the system. In Fig.10 we report for $\rho = 0.95 \text{ g/cm}^3$ isochore also the results obtained for a different configuration of soft spheres. As it can be seen changing the soft spheres position does not alter significantly the values of the pressure. From the isochores also the behaviour of the TMD line can be extracted. In fact along the TMD line the coefficient of thermal expansion

$$\alpha_P = \frac{1}{V} \left(\frac{\partial V}{\partial T} \right)_P \quad (7)$$

goes to 0.

The thermal pressure coefficient

$$\gamma_V = \left(\frac{\partial P}{\partial T} \right)_V \quad (8)$$

is connected to the coefficient of thermal expansion by the following equation

$$\gamma_V = \frac{\alpha_P}{K_T}. \quad (9)$$

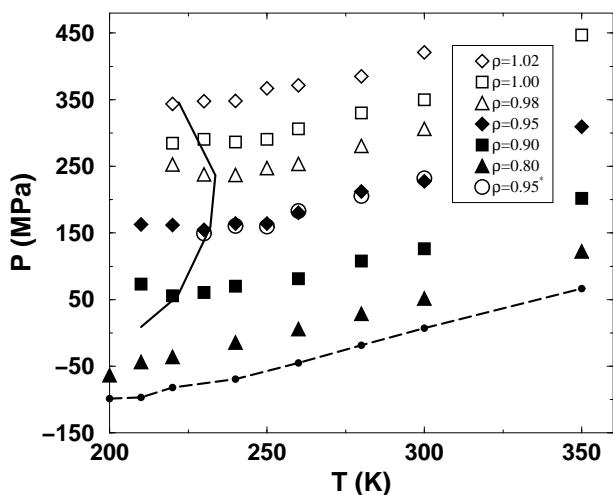


FIG. 10: $P_\rho(T)$ of the confined system isochores for several values of ρ in g/cm^3 , spinodal line (long dashed with points) and TMD curve (solid line). * Open circles represent the $\rho = 0.95 \text{ g/cm}^3$ isochore obtained from a different configuration of the matrix of soft spheres.

Therefore the TMD points lie on the line connecting the minima of the isochores. In the Fig. 10 also the TMD line is drawn. We observe, down to the lowest temperature investigated a non retracing spinodal and correspondingly a TMD that bends on approaching the spinodal. This behaviour is similar to both non polarizable⁶ and polarizable¹³ bulk TIP4P water. The interesting feature is represented by the shift induced by confinement on both the spinodal and the TMD with respect to the bulk. To give a more quantitative insight on this displacement we plotted in Fig.11 the isochores and the TMD for the

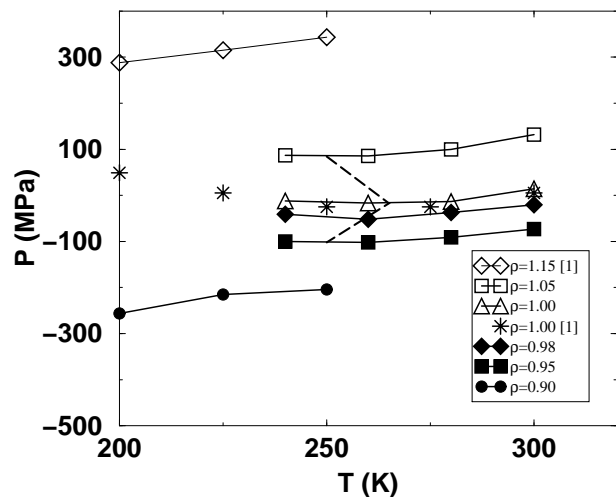


FIG. 11: $P_\rho(T)$ of the bulk system isochores for several values of ρ in g/cm^3 , TMD curve (long dashed line). The isochore of the lowest density is close to the spinodal.

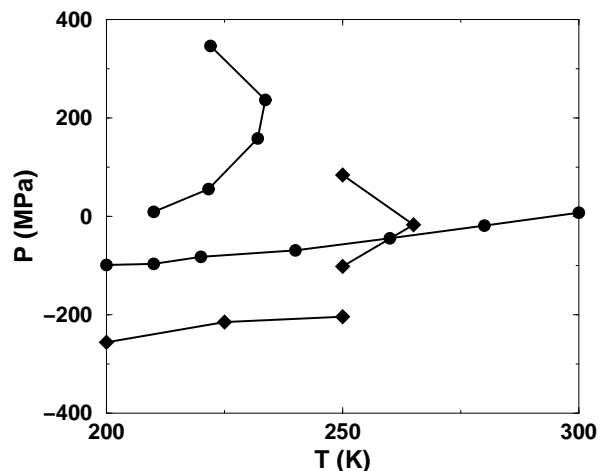


FIG. 12: TMD and spinodal of the confined system (bold lines with filled circles) and TMD and isochore of the lowest density for the bulk system (bold lines with filled diamonds).

bulk TIP4P. Some of the isochores have been calculated here as they are not available in literature. By comparing the spinodal and TMD curves of the bulk and confined system, Fig.12, we note that both the spinodal line and the TMD for water under hydrophobic confinement are shifted toward higher pressures. The TMD line shifts also to lower temperatures and correspondingly its curvature broadens. In a different hydrophobic confinement²², as already quoted in the introduction, a negative shift of 40 K has been observed with respect to the bulk for the TMD, but no shift in pressure nor changes in the curvature were found. Interestingly our shift in temperature is also roughly 40 K.

V. CONCLUSIONS

We performed a MD study of TIP4P water confined in a rigid matrix of soft spheres. The geometry of the hydrophobic environment in our case is different with respect to the previous studies mentioned above where water is confined between plane surfaces. We observed that the effect on water structure is similar to the case of a solution of small apolar solutes when it is taken into account that the decrease of water density is equivalent to an increase of solute concentration. Moreover we found that volume excluded effects reduce the average number of hydrogen bond, The hydrogen bond network however

is preserved at variance with the case of water confined in hydrophobic plates.

In spite of the preservation of the network of water and the not large changes in its structure we observe an important shift of the limit of stability both in pressures and temperatures and also a different shape in the shifted TMD with respect to the bulk. The temperature shift similar to the one observed by Kumar et al.²². These simulation indicate only a weak dependence of water properties on the confining potential¹⁷. It would be therefore valuable to understand to what extent an analogy can be drawn.

-
- ¹ O. Mishima and H. E. Stanley, *Nature* **396**, 329 (1998).
² P.H.Poole, F.Sciortino, U.Essman and H.E.Stanley, *Nature* **360**, 324 (1992);
³ See P.G. Debenedetti, *J. Phys.: Condens. Matt.* **15**, R1670 (2003) and references therein.
⁴ P. G. Debenedetti and H. E. Stanley, *Phys. Today* **56**, 40 (2003).
⁵ R.J. Speedy, C.A. Angell, *J. Phys. Chem.* **65**, 851 (1976); R. Speedy, *J. Phys. Chem.* **86** 982 (1982); *ibid* **86**, 3002 (1982).
⁶ P.H.Poole, F.Sciortino, U.Essman and H.E.Stanley, *Phys. Rev. E* **48**, 3799 (1993)
⁷ F. Sciortino, P.H. Poole, U. Essmann and H. E. Stanley, *Phys. Rev. E* **55**, 727 (1997).
⁸ P. H. Poole, I. Saika-Voivod and F. Sciortino *J. Phys. Condens. Matter* **17**, L431 (2005).
⁹ H. Tanaka, *J. Chem. Phys.* **105**, 5099 (1996).
¹⁰ S. Harrington, P.H. Poole, F. Sciortino and H.E. Stanley, *J. Chem. Phys.* **107**, 7443 (1997).
¹¹ P. A. Netz, F. W. Starr, H. E. Stanley and M. C. Barbosa, *J. Chem. Phys.* **115**, 344 (2001).
¹² M.Yamada, S. Mossa, H.E. Stanley, F.Sciortino, *Phys. Rev. Lett.* **88**,195701 (2002)
¹³ P. Gallo, M. Minozzi and M. Rovere, *Phys. Rev. E* **75**, 011201 (2007).
¹⁴ S. Sastry, P.G. Debenedetti, F. Sciortino and H. E. Stanley *Phys. Rev. E* **53** 6144 (1996).
¹⁵ N. Giovambattista, P. G. Debenedetti and P. J. Rossky, *J. Phys. Chem. C* **111**, 1323 (2007).
¹⁶ M. C. Gordillo and J. Marti, *Phys. Rev. B* **75**, 085406 (2007).
¹⁷ P. Kumar, F. W. Starr, S. V. Buldyrev and H. E. Stanley, *Phys. Rev. E* **75**, 011202 (2007).
¹⁸ N. Giovambattista, P. J. Rossky and P. G. Debenedetti, *Phys. Rev. E* **73**, 041604 (2006).
¹⁹ H. Jansson, W. S. Howells, J. Swenson, *J. Phys. Chem. B* **110** 13786 (2006).
²⁰ C. Corsaro, V. Crupi, D. Majolino, P. Migliardo, V. Venuti, U. Wanderlingh, T. Mizota, M. Telling, *Mol. Phys.* **104** 587 (2006).
²¹ S.-H. Chen, F. Mallamace, C. Y. Mou, M. Broccio, C. Corsaro, A. Faraone and L. Liu, *Proc. Nat. Acad. Sci. USA* **103**, 12974 (2006).
²² P. Kumar, S. V. Buldyrev, F. W. Starr, N. Giovambattista and H. E. Stanley, *Phys. Rev. E* **72**, 051503 (2005).
²³ J. Puibasset, R. J. M. Pellenq, *J. Chem. Phys.* **122**, 094704 (2005).
²⁴ L. Liu, S.-H. Chen, A. Faraone, C. W. Yen and C. Y. Mou, *Phys. Rev. Lett.* **95**, 117802 (2005).
²⁵ A. Faraone, L. Liu, C. Y. Mou, C. W. Yen and S.-H. Chen *J. Chem. Phys.* **121**, 10843 (2004).
²⁶ P. Gallo, M. Rapinesi and M. Rovere, *J. Chem. Phys.* **117**, 369 (2002).
²⁷ P. Gallo, M.A. Ricci and M. Rovere, *J. Chem. Phys.* **116**, 342 (2002).
²⁸ T. M. Truskett, P. G. Debenedetti and S. Torquato, *J. Chem. Phys.* **114**, 2401 (2001).
²⁹ P. Gallo, M. Rovere, E. Spohr, *Phys. Rev. Lett.* **85**, 4317 (2000).
³⁰ P. Gallo, M. Rovere, E. Spohr, *J. Chem. Phys.* **113**, 11324 (2000).
³¹ M. Meyer, H. E. Stanley, *J. Phys. Chem B* **103** 9728 (1999).
³² K. Koga, X. C. Zeng and H. Tanaka, *Phys. Rev. Lett.* **79**, 5262 (1997).
³³ Limei Xu, Pradeep Kumar, S. V. Buldyrev, S.-H. Chen, P. H. Poole, F. Sciortino and H. E. Stanley, *Proc. Nat. Acad. Sci. USA* **102**, 16558 (2005).
³⁴ K. Lum, D. Chandler and J. D. Weeks, *J. Phys. Chem. B* **103**, 4570 (1999).
³⁵ D. Chandler, *Nature* **437**, 640 (2005).
³⁶ W. L. Jorgensen, J. Chandrasekhar, J. D. Madura, R. W. Impey and M. L. Klein, *J. Chem. Phys.* **79**, 926 (1983).
³⁷ L.R. Pratt and D. Chandler, *J. Chem. Phys.* **67**, 3683 (1977).
³⁸ G. Graziano, *J. Chem. Soc, Faraday Trans.* **94**, 3345 (1998).
³⁹ B. Guillot and Y. Guissani, *J. Chem. Phys.* **99**, 8075 (1993).
⁴⁰ V. De Grandis, P. Gallo and M. Rovere, *J. Chem. Phys.* **118**, 3646 (2003).
⁴¹ P. Cristofori, P. Gallo and M. Rovere, *Mol. Phys.* **103**, 501 (2005).

